



India-Asia collision was at 24°N and 50 Ma: palaeomagnetic proof from southernmost Asia

Jun Meng¹, Chengshan Wang¹, Xixi Zhao², Rob Coe², Yalin Li¹ & David Finn²

¹State Key Laboratory of Biogeology and Environmental Geology (China University of Geosciences), Beijing 100083, China, ²Department of Earth and Planetary Sciences, University of California, Santa Cruz, CA 95064, USA.

SUBJECT AREAS:
PALAEOMAGNETISM
TECTONICS
GEOLOGY
PALAEOCLIMATE

Received
17 September 2012

Accepted
14 November 2012

Published
5 December 2012

Correspondence and
requests for materials
should be addressed to
C.W. (chshwang@
cugb.edu.cn)

How and when India collided with Asia is crucial for global climate and continental dynamics. We present new palaeomagnetic data showing that the Xigaze forearc basin of southern Tibet was located at $24.2 \pm 5.9^\circ\text{N}$ during 54–57 Ma, providing a direct constraint on the position of the southernmost margin of Asia at this crucial stage. Our study suggests 1) the age and locus of the initial India-Asia collision are at ~ 50 Ma and $\sim 24^\circ\text{N}$, respectively; 2) Tibet resisted India's northward push during the first ~ 16 Ma of initial impact from the collision and experienced little latitudinal displacement; and 3) Sometime a little after 34 Ma, Greater India was consumed and thicker Indian Craton subsequently made contact with Asia, resulting in $\sim 6^\circ$ northward drift of Asia. Our model has implications for the process by which the high proto-Tibetan plateau formed and for the two slowdowns of India's convergence rate with Asia.

The uplift histories of high plateaus are very important for understanding global climatic changes and continental dynamics. In particular, the Tibetan Plateau, which is well known as the 'roof' of the world, has attracted much attention because of its high elevation, large size, and striking flatness¹. Tibet mainly consists of three tectonic terranes: from north to south the Songpan-Ganzi, Qiangtang and Lhasa terranes, which accreted successively to Eurasia since the Early Mesozoic². Later, during Cenozoic time¹, the India-Asia collision occurred, contributing to the uplift of the Tibetan Plateau and also deforming large parts of Asia^{2–4}. The uplift of the Tibetan Plateau may have triggered the trend of decreasing atmospheric CO₂ concentration and major change in global climate in Eocene⁵.

The Yarlung Zangbo suture in south central Tibet marks the contact between the Lhasa terrane (Asia plate) to the north and the Tethyan Himalaya terrane (Indian plate) to the south (Fig. 1a). It is generally regarded as the remnant of the Neo-Tethys Ocean and consists of four major tectonic units (from north to south): the Cretaceous-Tertiary Gangdese magmatic arc, the Xigaze forearc basin, an ophiolite belt and the accretionary wedge containing Permian-Eocene rocks⁶. The Xigaze forearc basin formed at the southernmost continental (Andean) margin of Eurasia⁷ and probably extended along the entire southern margin of the Lhasa terrane, representing the southernmost leading edge of Asia. Documented relics of the forearc basin at the present day are located between the subduction zone and the Gangdese belt and have a length of ~ 660 km and width of ~ 20 km (Fig. 1a). It was shortened by about 35–65% after the collision⁸, which is a minimum estimate because part of the forearc has been underthrust below the Lhasa terrane. The basin fill consists of Cretaceous-Palaeogene sedimentary deposits that were contributed from sources to the north in the Lhasa terrane^{6–8} until the terminal forearc stage, which is represented by the Late Cretaceous-Early Palaeogene shallow marine sediments⁶.

Despite more than three decades of active research, the lack of consensus regarding the timing of the collision^{2,9–14} and the tectonic processes by which the Tibetan Plateau was raised¹ hinders understanding of the dynamic processes governing the kinematic history and structural development of Asia. Published palaeomagnetic studies have inferred inconsistent palaeolatitudes for the southern margin of Asia, which is the main cause for the wide range of collision ages (20–70 Ma)^{9,12,13,15–21}, as well as post-collisional shortening estimates, which range from a couple hundred kilometers to ~ 2000 km^{9,19}. Van Hinsbergen *et al.* (2012) recently presented a compilation of palaeomagnetic data from Lhasa and Tethyan Himalaya terranes¹³ showing a two-stage India-Asia collision at ~ 52 and 25–20 Ma. Although this compilation is a timely service, the new tectonic scenario has been hotly debated^{22,23}. These models use geophysical and geologic records between Lhasa and the Tethyan Himalaya terranes to constrain the India-Asia collision and lack a more direct measure of the collision, such as the coeval palaeolatitudes of Asia's southernmost and India's northernmost margins.

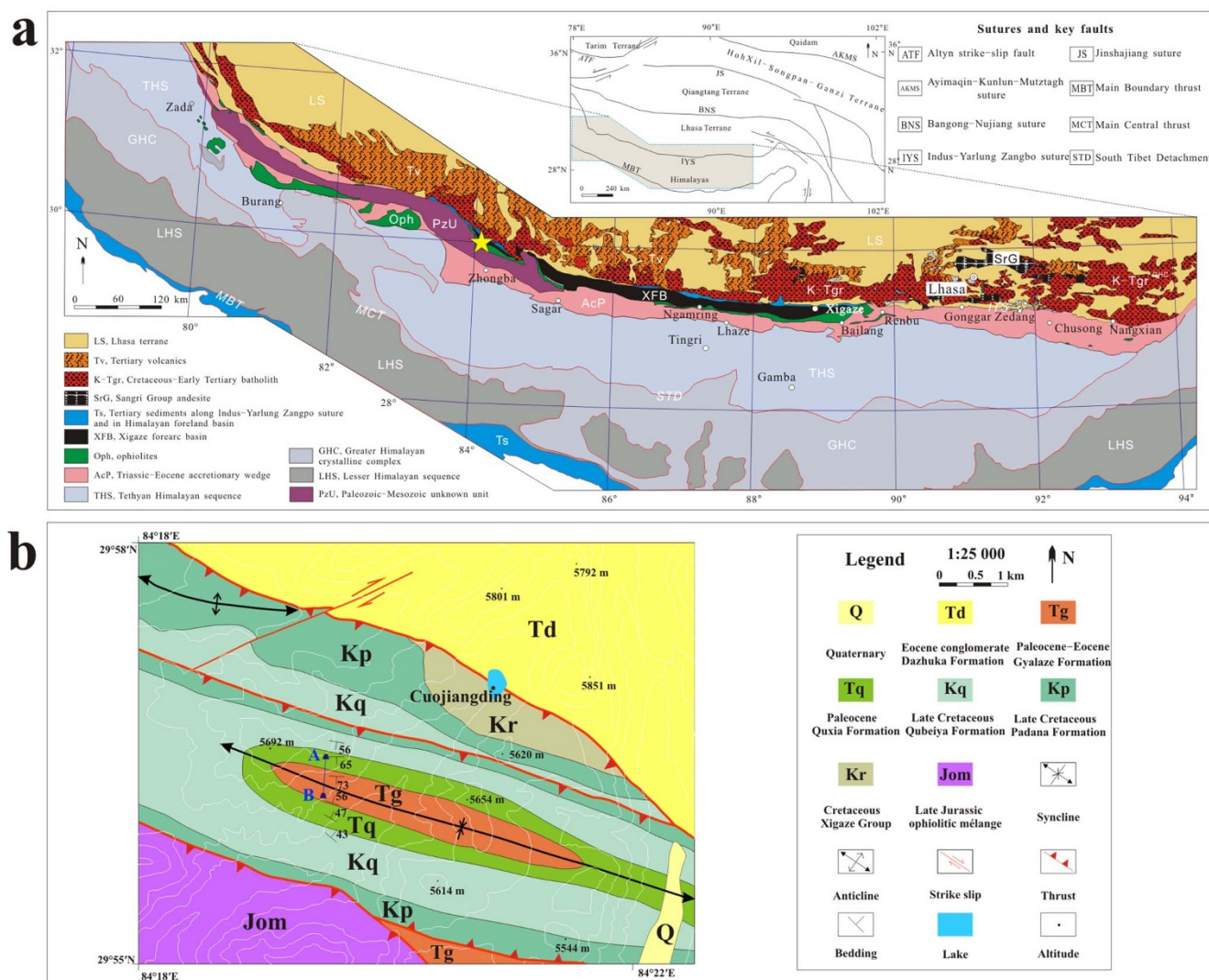


Figure 1 | Sketches of geology and sampling location for this study. (a), Geological map of the Western Indus-Yarlung Zangbo (IYZ) suture zone showing the position of Xigaze forearc basin and palaeomagnetic sampling area for this study (yellow star). Insert: present location of tectonic terranes in Tibet and surrounding regions; (b), Updated geological map of the study area by us, showing our palaeomagnetic sampling sites (A–B section) are located at the southernmost margin of the Asian plate.

In an effort to provide constraints to resolve these questions, we carried out a geological and palaeomagnetic study of the Xigaze forearc basin in the Cuojiangding area of Zhongba County (29.9°N, 84.3°E) of southern Tibet (Fig. 1). The sedimentary sequences of the Xigaze forearc basin are characterized by the flysch-dominated Xigaze Group and shallow marine Cuojiangding Group (Fig. 1b). The strike of well bedded Cuojiangding Group strata is approximate W–E. The Cuojiangding Group and the Xigaze Group strata were deformed by kilometer-scale synclinal folds, which are intersected by east-west trending Gangdese thrust structures. The Gangdese thrust fault cut and placed the Xigaze and Cuojiangding Groups in the hanging wall and transported them southward over the Late Eocene-Miocene conglomerates^{14,24,25}. The timing of slip on the Gangdese thrust has been inferred between 30 and 23 Ma²⁵. The Late Eocene-Miocene conglomerates were not folded. Thus, folding must have occurred during the Eocene, enabling a palaeomagnetic fold test on the age of magnetization.

The Cuojiangding Group consists of the Padana, Qubeiya, Quxia, and Gyalaze Formations (Fig. 2). In the area we studied, the Quxia Formation is ~80 m thick and is dominated by conglomerates with sandstone intercalations. The Gyalaze Formation is >120 m thick and composed of gray to dark gray foraminiferal sandy limestone

and lithic sandstone. Well-lithified volcanic tuff layers occur near the middle part of the Gyalaze Formation, affording radiometric dates to further constrain the age of formation (54.8 ± 0.7 Ma, Dr. Xiumian Hu, personal communication). Geochronologic investigations using U-Pb zircons²⁵ and fossils^{6,26} also show that the age of the Gyalaze Formations is 50–60 Ma (Fig. 2).

We collected 130 oriented palaeomagnetic samples from the Palaeocene Quxia and Eocene Gyalaze Formations of the upper Cuojiangding Group using a gasoline-powered drill. The main lithology of our samples is gray sandstone, sandy limestone and tuff. The samples were distributed along the northern and southern limbs of a syncline (Fig. 1b). Where possible, samples were oriented using both magnetic and sun compasses.

Results

Rock magnetic results. A clear decrease in the heating curves during the temperature versus susceptibility experiments shows that all samples tested have well-defined Curie temperatures between 560°C and 580°C (Supplementary Fig. S1). The susceptibility during cooling displays the same Curie temperature and is only slightly higher than that during the heating. These characteristics show that the main magnetic mineral is magnetite and does not

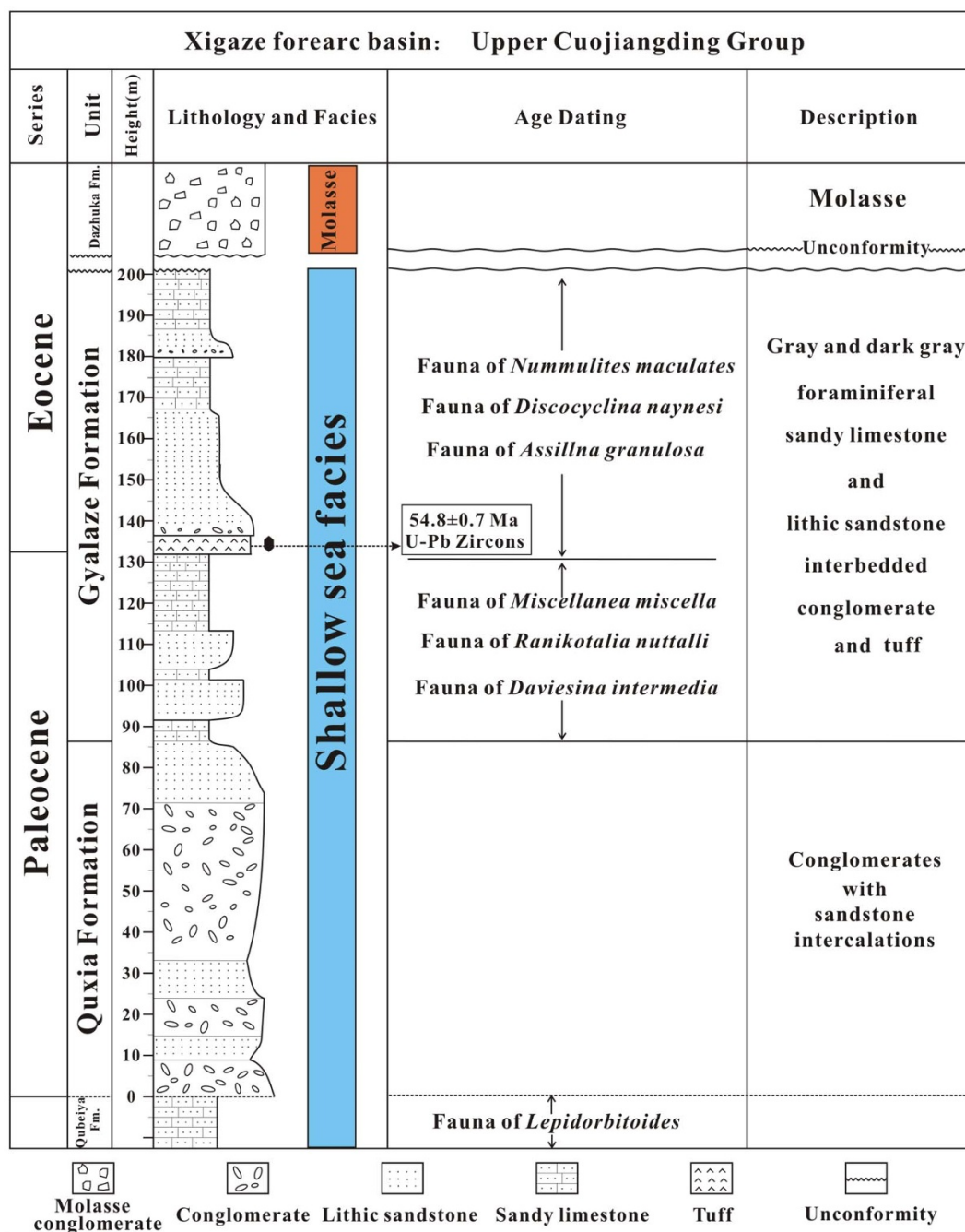


Figure 2 | Stratigraphic column showing lithofacies and age dating. The fossil record is after Wang *et al.* (2011)⁶. Zircon U-Pb age of Gyalaze Formation is from Dr. Xiumian Hu (personal communication).

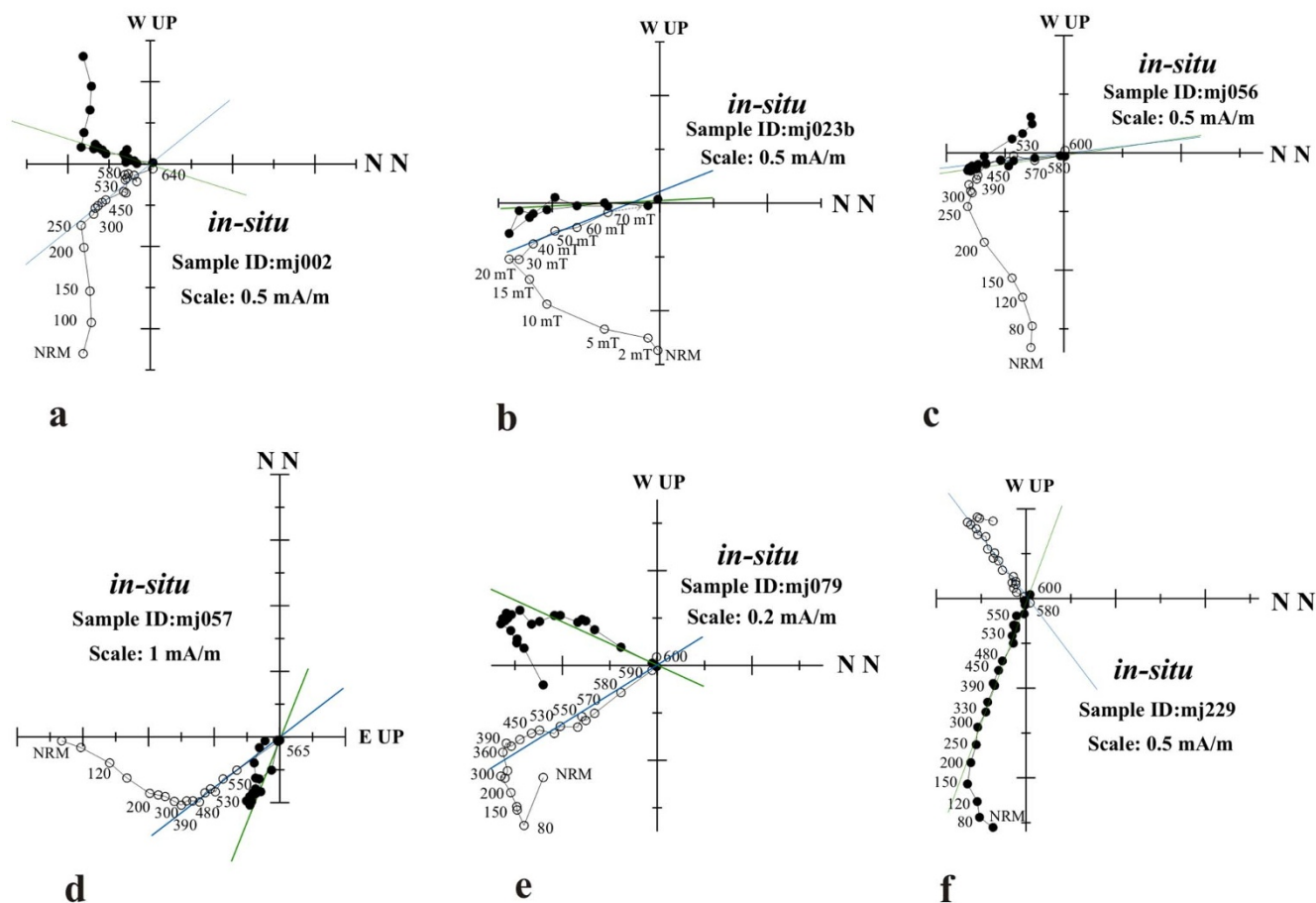
alter significantly during heating. Squareness (M_{rs}/M_s) and coercivity ratios (H_{cr}/H_c) obtained in the magnetic hysteresis measurements show that the mean magnetic grain size lies in the pseudo-single domain field of a Day plot^{27,28} (Supplementary Fig. S2).

Demagnetizations and palaeomagnetic directions. According to their demagnetization behavior, we assigned 4 grades to all the samples from the upper Cuojiangding Group (Supplementary Table S1, Fig. 3, and Supplementary Fig. S3). Out of 130 samples, 31 samples were defined as grade A (= 'very good to excellent') (Fig. 3a–f). The natural remanent magnetization (NRM) of grade A samples is composed of two directional components. A high temperature component (HTC) is isolated that decays straight toward the origin, usually in the 450–590°C interval, indicating

that the main magnetic carrier is magnetite and that this HTC is the characteristic remanent magnetization (ChRM). Several samples treated by alternating field (AF) demagnetization also display ChRM directions consistent with those from thermal demagnetization (Fig. 3b). Thirty eight samples were defined as grade B (= 'OK and useful') (Fig. 3g–i). Their demagnetization behavior exhibited two or three directional components, but less clearly. The HTC component was observed at temperatures of 300–580°C and decayed with a distinct trend toward the origin, but not as smoothly as for grade A samples. Only several HTCs required heating above 590°C to isolate the ChRM (Fig. 3g). Thirty three samples were defined as grade C (= 'seems right but doubtful') (Supplementary Fig. S3a,b). Some of them exhibit a reversed intermediate unblocking temperature component (ITC) between



Palaeomagnetic demagnetization data-Grade A



Palaeomagnetic demagnetization data-Grade B

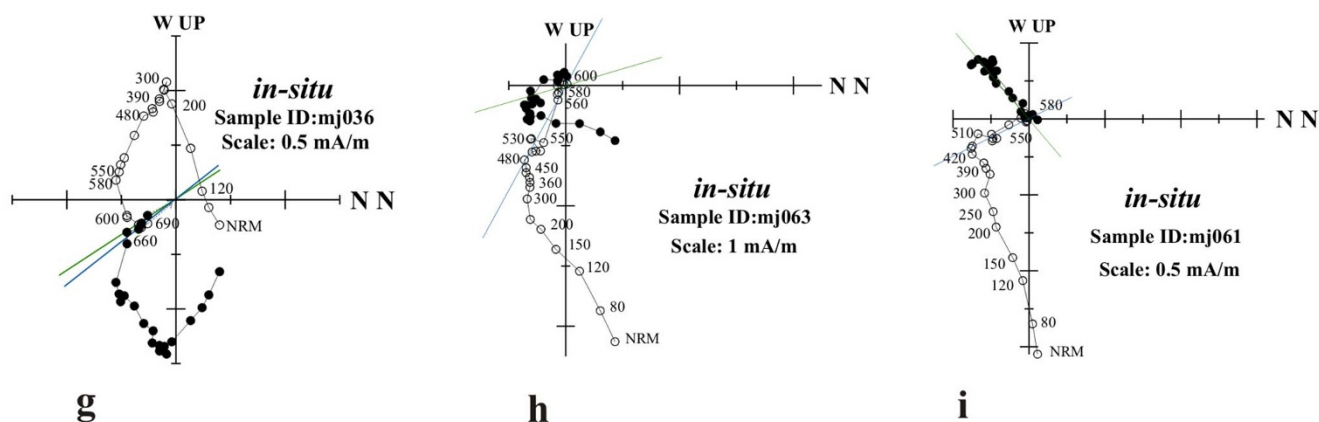


Figure 3 | Representative orthogonal projections of grades A and B palaeomagnetic demagnetization data from upper Cuojiangding Group plotted in *in-situ* coordinate. Solid (open) circles are the horizontal (vertical) plane projections. Scales are in mA/m. Straight lines represent the least-square-best fitting directions of the ChRM. See text for description of demagnetization behavior.

300 and 500°C that is a little shallower but agrees approximately with the mean HTC direction of grades A and B (Supplementary Fig. S3a). Samples with directions that can only be constrained by great circles (Supplementary Fig. S3b) also were labeled as grade C. Twenty eight samples were defined as grade D (=‘unacceptable’). These samples exhibited unstable directions that were unsuitable for applying principle component analysis to determine an HTC component

(Supplementary Fig. S3c). After all low-stability components of NRM have been removed, the remaining HTC components are only accepted as the ChRM if they exhibit linear trajectories of demagnetization towards the origin and a reasonably consistent *tilt-corrected* direction from sample to sample that is significantly different from the present-day field in *in-situ* coordinates. We only used A and B sample directions for the final results in this study.



Table 1 | ChRM mean directions of upper Cuojiangding Group

Mean direction	N	D _g	I _g	K _g	α _{95g}	D _s	I _s	K _s	α _{95s}	Grade
Mean direction of A	31	170.1	19.3	4.4	13.9	170.6	-40.9	8.7	9.3	A
Mean direction of B	38	163.7	18.9	3.3	15.2	166.9	-42.4	6.7	9.7	B
Mean direction of C	33	184.4	30.6	2.8	17.5	189.4	-35.5	3.5	15.2	C
A,B mean direction	69	166.7	19.2	3.8	10.2	168.6	-41.7	7.6	6.7	A+B
A,B,C mean direction	102	170.5	20.4	3.4	8.8	173.6	-41.1	5.7	6.4	A+B+C
mean direction used	62	167.4	22.0	4.0	10.4	168.1	-42.0	7.4	7.1	A+B no normal polarity samples

Note: N, number of samples used to calculate mean direction; D_g, I_g (D_s, I_s), directions in geographic (stratigraphic) coordinates; k_g/k_s, best estimate of Fisher's (1953) precision parameter for the mean direction indicating the degree of clustering in geographic/stratigraphic coordinates; α_{95g}/α_{95s}, the radius of circle around calculated mean that has 95% chance of true mean lies with it in geographic/stratigraphic coordinates.

All low temperature components (LTCs) of the upper Cuojiangding Group are north and down and distributed around the present-day field direction (Dec = 0.6°, Inc = 46.4°). They yield a mean LTC which is obviously a modern-field viscous overprint (D_g = 0.2°, I_g = 44.6°, k_g = 15.8, α₉₅ = 4.0°, n = 85, in geographic coordinates; D_s = 181.4°, I_s = 74.4°, k_s = 3.9, α₉₅ = 9.0°, n = 85, after tectonic correction, see Supplementary Fig. S4). We calculated the mean ChRM directions by grade as shown in Table 1. The very few ChRMs with normal polarity in *tilt-corrected* coordinates were inverted to reversed. Grades A and B samples have nearly the same mean direction, whereas the mean inclination of grade C samples is slightly shallower. The grade A mean direction has the largest precision parameter (k), and k decreases with the decline of reliability from grade A to C. To obtain a more accurate direction, all the C and D grade samples were excluded from further analysis. Finally, we remove the seven normal polarity directions from the formation mean because we suspect that they were remagnetized, albeit before tilting, as discussed below.

Reliability of the ChRM directions and site mean direction. We sampled the upper Cuojiangding Group moving stratigraphically from bottom to top and each individual sample direction in a different sedimentary layer defines a palaeomagnetic site. In the end we obtained 69 site directions in the upper Cuojiangding Group. They are scattered in geographic coordinates, the inclination especially differing (up or down) in the two opposing limbs of the fold, and clustering increases after applying the structural correction. The ratio of the Fisher (1953) precision parameter, k_s/k_g = 2.0 is larger than the critical value of 1.25–1.39 for 95% confidence²⁹, indicating that the ChRM was acquired prior to folding. Furthermore, a Direction-Correction fold test of Enkin (2003)³⁰ for the site mean directions also gives optimal untilting at 94.9 ± 14.3% and a positive test. In addition, using the test of McFadden (1990)³¹, the fold test results are positive at more than 99% confidence level (Supplementary Table S2): in *in-situ* coordinates, the value (22.043) of summation of cosine angles (SCOS), which was defined in Equation 14 of McFadden (1990)³¹, exceed the critical value (13.662) for the 99% confidence level. So there is a highly significant correlation between the ChRM directions and tectonics, and it is clear that the ChRM was acquired before tilting. Conversely, in the unfolded coordinates, the SCOS value (0.178) is far less than the critical value at 99% confidence level so the hypothesis that the ChRM was acquired before folding is tenable. Finally, according to geological evidence, the fold occurred during the Early Eocene, and thus we interpret the ChRM to be a primary remanence.

The directions of 55 sites from the north limb of the upper Cuojiangding Group were used to calculate the virtual geomagnetic pole (VGP) latitudes as a function of stratigraphic height in Fig. 4. The magnetic polarity sequence is dominated by reversed polarity with only four normal samples scattered among the reversed sites. The tuff bed shown near the middle of the stratigraphic column is dated at 54.8 ± 0.7 Ma, placing it squarely within C24r of the

geomagnetic polarity timescale (GPTS)³², an entirely reversed polarity-chron spanning the interval 53.8–56.6 Ma. Although it is possible that the few normal samples might indicate three or four undocumented normal polarity subchrons, we think it more likely that they are isolated instances of pre-tilting remagnetization in a later normal field (e.g., Chron C24n). The minimum sedimentation rate for the upper Cuojiangding Group assuming that it lies entirely within C24r is ~7 cm/ka, which is reasonable for shallow sea facies. Therefore, all seven normal samples were removed from the population in further analysis, even though retaining them has no significant influence on the mean direction for the section (Table 1). As a result, we obtain the site mean direction for ~54–57Ma (red bold italic in Table 1 and Fig. 5): D_s = 168.1°, I_s = -42.0°, k_s = 7.4, α₉₅ = 7.1°, n = 62 sites (after tectonic correction).

The number of samples is less than ideal for the Elongation/Inclination (E/I) method of Tauxe and Kent³³, so we do not make any such correction. However, our palaeomagnetic mean inclination (42° ± 7.1°) is consistent with that (40.3° ± 5.6°) for the coeval volcanic data from the upper Palaeocene to lower Eocene (56–47 Ma) Linzizong Group^{13,17}. Agreement of our inferred palaeolatitude with Lippert *et al.* (2011)'s results from volcanic rocks^{13,34} also supports this conclusion. For these reasons we conclude that our results from the upper Cuojiangding Group are not affected by inclination shallowing.

The palaeomagnetic pole calculated from these *tilt-corrected* sediments is located at 78°N, 329°E. The palaeolatitude of the sampling area (and thus the southernmost margin of this part of Asia) inferred from our palaeomagnetic data is 24.2° ± 5.9°N at ~54–57 Ma. Compared with today's position of the sampling area, the southernmost margin of Asia has moved 5.7 ± 5.9° northward since that time.

Discussion

The motion of India relative to stable Eurasia can be reconstructed from the history of seafloor spreading in the Indian and Atlantic oceans and the rifting in east Africa. Various tectonic reconstructions have assumed that the dramatic change of India's northward convergence velocity between 50 and 35 Ma (dropping from ~18 to ~5 cm/yr) represents the onset of the India-Asia collision^{9,10,35–37}. A more convincing, direct way to find out when India collided with Asia would be to determine when coeval palaeolatitudes of Asia's southern and India's northern margins first began to overlap. The overlap of the palaeolatitude curves derived from the Eurasian and Indian apparent polar wander paths (APWPs)³⁸ can't reflect the correct collision age because it occurs at less than 10 Ma (Fig. 6a), which is much too young. The likely reason is that shortening happened within the Asia and India plates, and these palaeolatitudes are based on the present day shape of the continents. Thus to construct palaeolatitude curves for the Indian and Asian margins it is important to use autochthonous palaeomagnetic data, that is data from as close to those margins as possible.

Based on new compilations^{12,13}, we review the palaeomagnetic data derived directly from the margin of Indian and Asian plates. Under

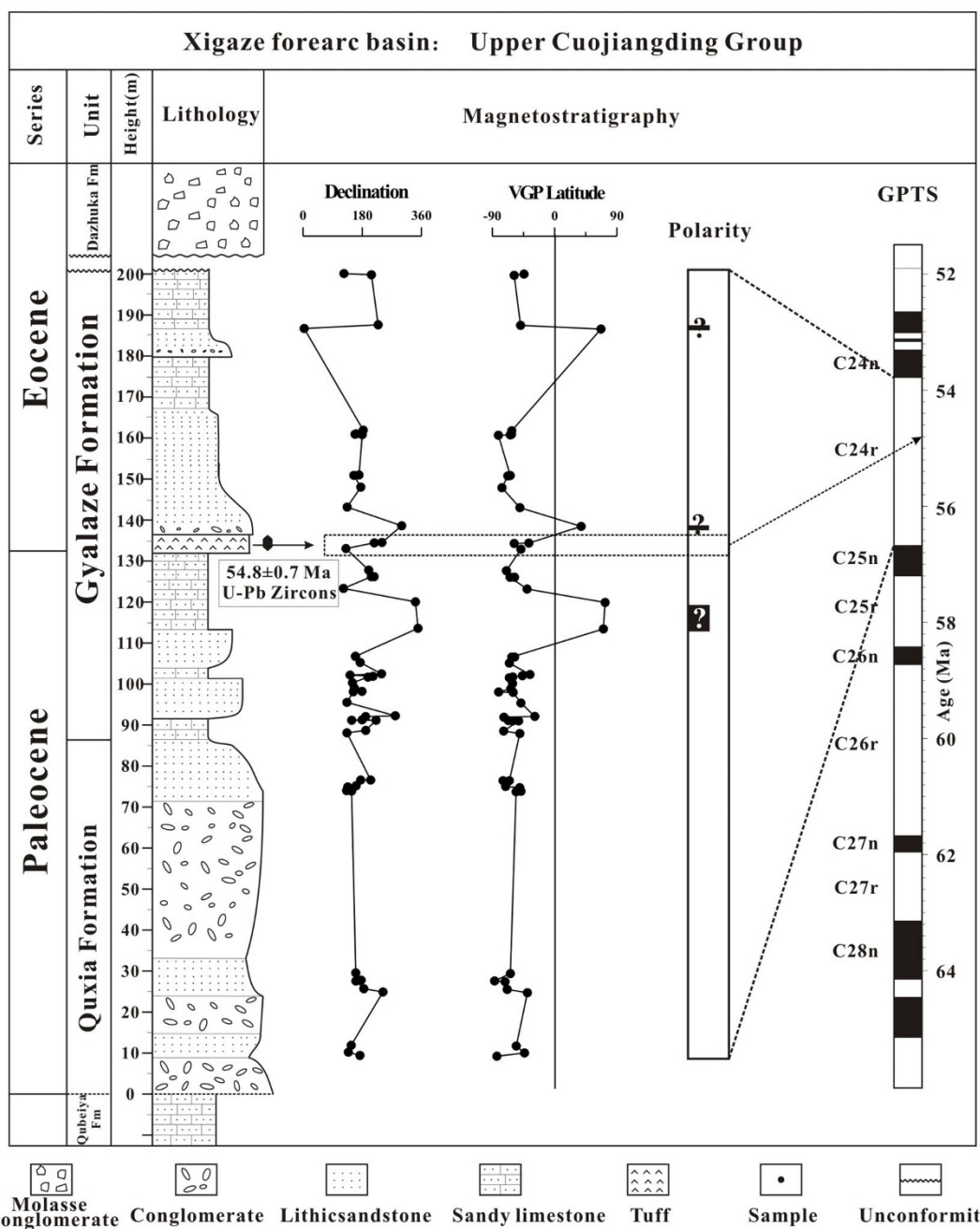


Figure 4 | Lithologic and magnetostratigraphic results from upper Cuojiangding Group in southern Tibet with declinations and VGP latitudes plotted as a function of stratigraphic level and showing the correlation with the GPTS³².

the premise of meeting the foremost rigorous palaeomagnetic criteria (a proven primary signal and well-determined age constraint)³⁹, we then add other palaeomagnetic reliability criteria (the correction of sedimentary inclination shallowing and averaging of palaeosecular variation (PSV) in volcanic-based data) to assess these individual poles. Together with our newest results, we extract robust palaeomagnetic data to construct palaeolatitudes of the Indian and Asian margins.

On the Indian side, Late Cretaceous to Eocene palaeomagnetic data directly from the northern margin of India are scarce. Supplementary Table S3 lists available palaeomagnetic results from the Late Cretaceous Zhongshan and Palaeogene Zongpu Formations in the Dingri and Gamba areas of Tethyan Himalayas^{40–43}. Cretaceous to Eocene marine strata in Dingri and Gamba areas of the Tethyan Himalaya represent the sedimentary development of the northern

continental margin of the Indian plate²⁴. Serious remagnetization in the Dingri area resulted in few sampling sites preserving primary remanence^{12,17,43}. Fortunately, recent palaeomagnetic results in the Gamba area of the Tethyan Himalaya (28.3°N, 88.5°E) yielded reliable concordant palaeolatitudes for the Indian-northernmost margin^{42,43}. Patzelt *et al.* (1996) reported that India possessed equatorial palaeolatitudes of 4.7°S±4.4° (65–71 Ma), 7.5°N±4.8° (63–66 Ma), and 4.8°N±3.8° (55–63 Ma), respectively⁴², which were not affected by significant inclination shallowing¹⁷. Yi *et al.* (2011) obtained higher resolution results from the same section with palaeolatitudes ranging from 6.6°N±3.5° (59–62 Ma) to 11.1°N±2.5° (56–59 Ma) in the lower and upper Zongpu formations⁴³. Positive fold and reversal tests indicated that the ChRM directions are primary remanence.

On the Asian side, Late Cretaceous data stem from studies of the Takena and Shexing Formations in southern Tibet (Supplementary

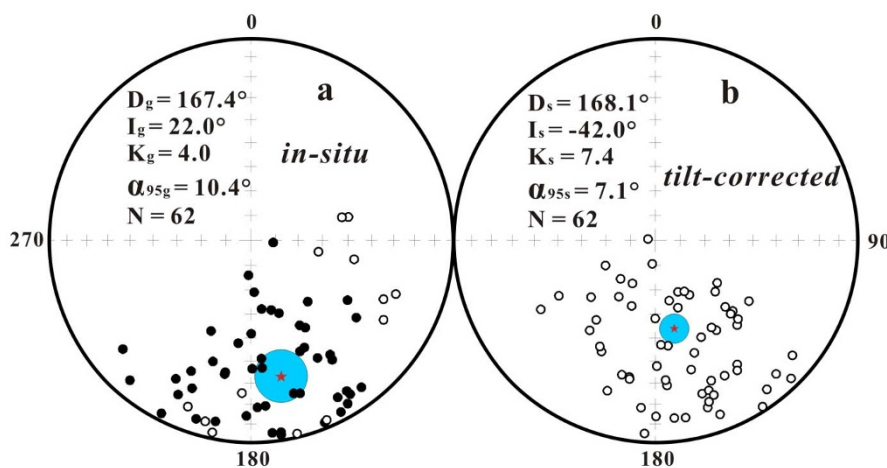


Figure 5 | Equal area stereonet projections of palaeomagnetic site directions from the upper Cuojiangding Group with a site mean direction (red black star, 95% confidence interval indicated in blue shadow): (a), *in-situ* site directions; (b), *tilt-corrected* site directions. Solid black circles indicate lower hemisphere projections and open black circles are directions in the upper hemisphere.

Table S4)^{15,19,21,44–46}, with palaeolatitudes ranging from $\sim 12^{\circ}\text{N}$ to $\sim 25^{\circ}\text{N}$ ¹². Basically, all these studies more or less agree with Tan *et al.* (2010)¹⁹ if large inclination shallowing is assumed. Tan *et al.* (2010) studied the Late Cretaceous redbeds of the Shexing formation (65–110 Ma) and volcanics intercalated within them (85–110 Ma) in the Linzhou area of southern Tibet (29.9°N , 91.2°E). The ChRM directions of both the redbeds and volcanics pass the fold test at 99% confidence and can be interpreted as primary remanence. Importantly, this study is the only one with enough intercalated lava flow samples to do a reasonable job of averaging PSV. The calculated pole dispersion $S_{\text{VGP}} = 14.9^{\circ}$ is consistent with known dispersion models for PSV: $S = 14.5^{\circ}$ in Johnson *et al.* (2008)⁴⁷ and $S = 12.5^{\circ}$ in Biggin *et al.* (2008)⁴⁸ for $\sim 21^{\circ}\text{N}$ of palaeolatitude, which is in agreement with that for the coeval redbeds corrected by the E/I method³³. This proves that E/I analysis correction is needed and works well for the Late Cretaceous redbeds of the Shexing formation. Other studies agree with Tan *et al.* (2010) when the inclination is corrected by E/I analysis¹³. To sum up, a palaeolatitude for the southern Asian margin of $\sim 25^{\circ}\text{N}$ is remarkably consistent for the reference point (29.9°N , 84.3°E) during Late Cretaceous time.

Most of the Tertiary results are from the Palaeogene Linzizong volcanic rocks in the same area on the Lhasa terrane (Supplementary Table S4). The Linzizong Group was classified into three formations (Dianzhong, Nianbo and Pana Formations) with accurate geochronological constraint ranging in age from 38 to 65 Ma⁴⁹. Palaeolatitudes derived from Linzizong Group are highly inconsistent and controversial^{12,13,15–20,45}. Nevertheless, Dupont-Nivet *et al.* (2010)¹⁷ and van Hinsbergen *et al.* (2012)¹³ compiled and synthesized palaeomagnetic results from the Linzizong volcanics, making the case that the results probably averaged out the PSV because of the large numbers of volcanic sites, and obtaining an average palaeolatitude quite close to that from our sediments.

Palaeomagnetic data from numerous Late Eocene lava flows (~ 34 Ma) of the Qiangtang terrane³⁴ also appear to have averaged out PSV reasonably well, the calculated pole dispersion agreeing with that expected for palaeosecular variation⁴⁷. Their palaeomagnetic pole gives a palaeolatitude of $28.7 \pm 3.7^{\circ}\text{N}$ for a reference point at $\sim 33^{\circ}\text{N}$, $\sim 88^{\circ}\text{E}$. When transferred to the southern margin of Asia (29.9°N , 84.3°E), these Eocene volcanic results suggest a palaeolatitude of $25.6 \pm 3.8^{\circ}\text{N}$ for 32–38 Ma assuming that the amount of N-S crustal shortening or rotation within the Lhasa terrane during Neogene time can be ignored¹³. Compared with our results, the palaeolatitude difference of Tibet between ~ 50 Ma and ~ 34 Ma is $1.4 \pm 5.9^{\circ}$, which indicates negligible to at most modest latitudinal

displacement of southernmost of Asia considering the error. Thus, this synthesis of recent palaeomagnetic results including our own data described above, derived from different parts of Tibet and depicted by the red dashed line in Fig. 6a, shows that the palaeolatitude of the southern margin of Asia was remarkably consistent around 24 – 25°N , moving almost imperceptibly northward from Late Cretaceous to Late Eocene time.

Across the suture zone, palaeolatitudes for the northernmost Indian margin increase progressively with decreasing age from $4.3^{\circ}\text{S} \pm 4.4^{\circ}$ at ~ 65 – 71 Ma, to $7.2^{\circ}\text{N} \pm 3.5^{\circ}$ at ~ 59 – 62 Ma, to $11.9^{\circ}\text{N} \pm 2.5^{\circ}$ at ~ 56 – 59 Ma for the reference point (29.9°N , 84.3°E)^{12,13,17,42,43}. This northward drift of the Indian margin, indicated by the green dashed line in Fig. 6a, is not exactly parallel to the blue solid line derived from the Indian APWP (Fig. 6a). If significant, the divergence in the lines would imply that extension was occurring in continental India during the Cenozoic until the time of collision. Van Hinsbergen *et al.* (2012) champion the role of very large extension commencing in the Early Cretaceous¹³. We do not choose to speculate beyond the Cenozoic time frame of our study, but simply note that the discrepancy in the two palaeolatitude lines indicates that the margin of Greater India at the time of collision lay ~ 1500 km or more to the north of the Indian Craton than it does today.

In Fig. 6a extrapolation of the palaeolatitude drift green-dashed line shows that the Indian margin at the 56–59 Ma time mark still needed to move $\sim 13^{\circ}$ farther north before reaching the Asian margin (indicated by the red dashed line). The intersection of the two palaeomagnetically determined drift lines gives the time of initial collision as well as its palaeolatitude. Using this configuration for pre-collisional Asia and India and the uncertainties shown in Fig. 6a, the best estimate for the age of initial collision is 49.7 Ma with upper and lower 95% confidence bounds of 44.3 and 55 Ma. The Gyalaze Formation (Fig. 2) marks the cessation of the marine strata along the suture zone and has been dated at ~ 50 Ma⁶, suggesting that the ocean between India and Tibet was closed and continental collision had started. Therefore, the ~ 50 Ma onset collision age is constrained by both palaeomagnetic and sedimentary studies from the same strata.

Based on this kinematic and other supporting evidence, we propose a tectonic model for the India-Asia collision (Fig. 7). The northern edge of Greater India was around latitude 7°N at ~ 60 – 62 Ma (Fig. 7a)⁴³. The widespread Cretaceous limestone and sandstone covering most of southern Tibet¹ indicate that it was a stable platform when these sediments were deposited. At around 57.5 Ma, Greater

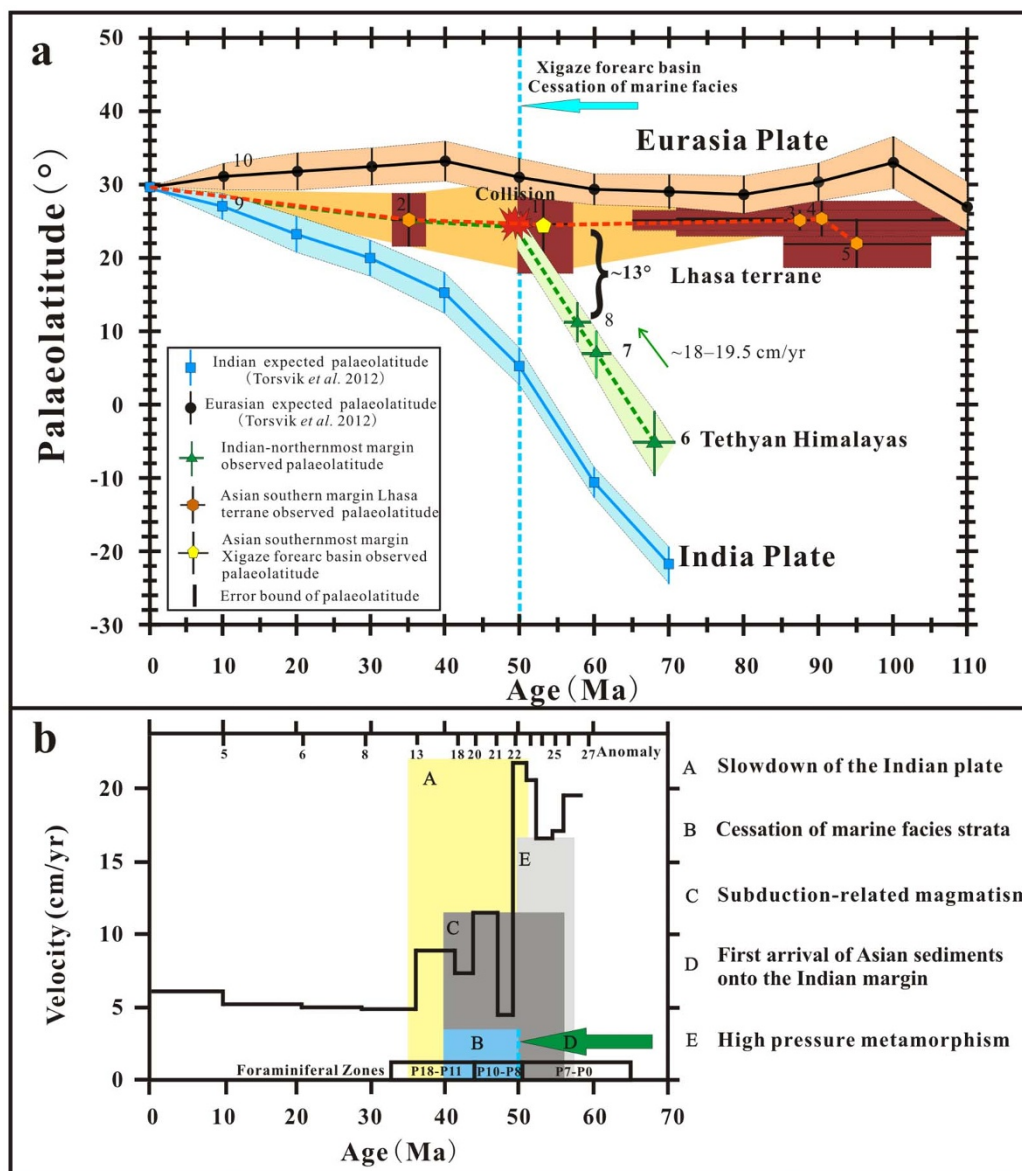


Figure 6 | Plots of palaeolatitudes and related geologic evidence for India-Asia collision. (a), Palaeolatitudinal comparison between the Asian and Indian margins (reference site, 29.9°N, 84.3°E). (b), Rate of convergence between India and Asia⁹ and other geological evidence for collision. Note: In (a), number '1' represents palaeolatitude for the Asian southernmost margin with 95% confidence limits on age and palaeolatitude from this study. Similarly, numbers '2, 3, 4, 5' are for the south Lhasa terrane margin: '2' is from upper Palaeogene volcanics results^{13,34}, '3' and '5' are from Late Cretaceous E/I corrected redbeds (65–110 Ma)¹⁹ and volcanics intercalated with sediments¹⁹, and '4' is from Late Cretaceous E/I corrected redbeds (72–100 Ma)¹³. Numbers '6, 7, 8' indicate palaeolatitudes and uncertainties for the Himalayas estimated from autochthonous palaeomagnetic results isolated from the Zongshan (~65–71 Ma)⁴², lower Zongpu (~59–62 Ma) and upper Zongpu (~56–59 Ma) Formations⁴³, respectively. Numbers '9' and '10' are the palaeolatitude curves for the southern margin of Eurasia (reference site, 29.9°N, 84.3°E) and the northern margin of India (reference site, 29.9°N, 84.3°E) derived from the Eurasian and Indian apparent polar wander paths of Torsvik *et al.* (2012)³⁸. Numbers correspond to palaeomagnetic poles and palaeolatitudes listed in Supplementary Table S5. Confidence limits are illustrated as black dashed lines. Red and green lines stand for the southern and northern margins of Asia and India, respectively. In (b), 'A–E' represent important geologic events during the collision. See text for details.

India was drifting northward at a velocity of ~18–19.5 cm/yr¹⁰ and the palaeolatitude difference between the Indian and Asian margins was ~13° (Fig. 7b). At ~50 Ma, the palaeolatitude difference reached zero at ~24°N, marking the initial continent-continent collision between India and Asia (Fig. 7c). With estimated subduction rates of ~7–8 cm/yr^{35,37}, the thinner non-cratonic part of Greater Indian margin (with a width ~1500 km) could have been almost entirely consumed by ~34 Ma. Thickened and uplifted Tibet¹ resisted thinned Greater India's northward subduction⁵⁰ during the first ~16 Ma of initial impact from the collision and experienced little latitudinal displacement, as reflected by the palaeolatitude data

(Fig. 7d). Probably by the end of the Eocene (~34 Ma) or a little later, the thicker Indian Craton⁵⁰ and Asia made contact, increasing compressional stress on the Asian plate⁵⁰ and resulting in ~6° shortening or northward drifting of Asia to the present position (Fig. 7e). This model better explains the onset of Indochina extrusion by ~20–35 Ma⁵¹ and may also have led to the two reductions in convergence rate of India with Asia at 45–40 Ma and at 20–10 Ma deduced by Molnar and Stock (2009)³⁷.

Our model agrees in age and palaeolatitude of collision with van Hinsbergen *et al.*'s model for Tibetan-Himalayan microcontinent-Asia collision¹³, but differs considerably in the pre-collisional

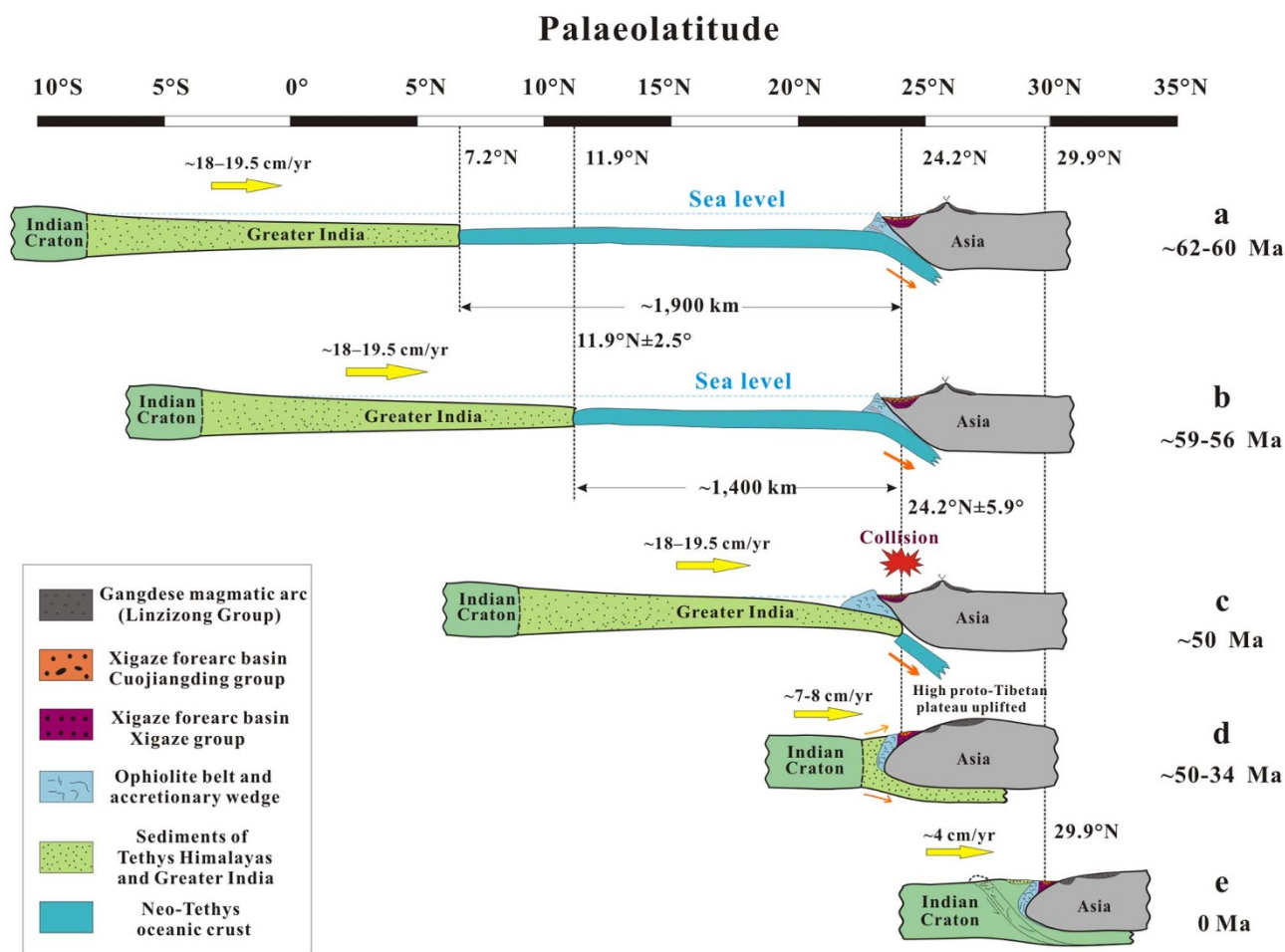


Figure 7 | Model showing the kinematic and dynamic evolution of the India-Asia collision. See text for details.

configuration of Greater India and post-collisional kinematic reconstructions. We describe these differences below.

Because no suture zone has been identified to suggest Tethyan Himalaya was ever a terrane separate from Indian continent⁵², reconstructions^{42,43} based on the same Palaeocene results from the Tethyan Himalaya used in our model have proposed a large northern extent of continental Greater India (~1500 km) since Late Cretaceous. In addition, new palaeomagnetic results from the Tethyan Himalaya also suggest >1300 km northern dimension of Greater India since Triassic⁵². Thus, in our model we start with a large continental Greater India for the pre-collision configuration of India. In contrast, by analyzing the Early Ordovician to Palaeocene palaeomagnetic poles for India, van Hinsbergen *et al.* (2012)¹³ propose that ~2500 km of N-S Cretaceous extension occurred within Greater India while the Tibetan Himalayan microcontinent rifted away from India in the Cretaceous by opening an oceanic Greater India Basin. Furthermore, in our model the palaeolatitude difference of Tibet between ~50 Ma and ~34 Ma is $1.4 \pm 5.9^\circ$. This probable near-standstill in palaeolatitude suggests that the continental convergence was mainly accommodated by the subduction and consumption of the Indian continental crust during this interval. Van Hinsbergen *et al.*, on the other hand, propose in their model that subduction of their extended oceanic Greater Indian Basin continued significantly later, until ~23 Ma.

In our kinematic reconstructions, the convergence history can be matched by numerical models⁵⁰ showing that two stage subduction of the denser thinned Greater India and thicker cratonic India and are in agreement with geological and geophysical observations.

India's northward convergence as indicated by analysis of sea-floor magnetic anomalies slowed markedly around Anomaly 21-22^{9,10,35,37} (48-50 Ma, Fig. 6b-A). The Eocene age of the last sedimentary marine facies dated as foraminiferal zones P8-P12 across the Himalayan belt¹¹ (Fig. 6b-B) correlates well with the initial stage of collision. Evidence for subduction-related magmatism¹ (Fig. 6b-C) and the first arrival of sedimentary material from Asia onto the Indian continental margin⁵³ (Fig. 6b-D) also corresponds with the timing of initial India-Asia collision at ~50 Ma. In addition, ultrahigh-pressure rocks formation and exhumation currently exposed in the Himalayas dated between 57-50 Ma⁵⁴ (Fig. 6b-E), suggesting the onset of Indian continental subduction below Asia during this time interval.

The standstill feature of the Tibetan Plateau in our model during the first ~16 Ma of the collision is also consistent with some geologic and geophysical evidence in the region. During ~50-34 Ma, the existence of thickened high proto-Tibetan plateau¹, the significant eastward shift (~40°) of the Euler pole for India, and the rearrangement of the plate boundary in the Indian Ocean³⁵ all favor the hypothesis that a large part of Greater India thrust beneath Tibet and thickened the crust by mechanical coupling⁵⁵.

In conclusion, the kinematic model, based on our palaeomagnetic results establishing the palaeolatitude of the southern margin of Asia and on other palaeomagnetic and geological evidence, shows that Greater India was converging with the southern margin of Eurasia in Tibet at a palaeolatitude of ~24°N and began to collide at around 50 Ma. For about the next 16 Ma the southern margin of Asia remained almost fixed while thinner Greater India was subducting



and causing shortening in the Himalaya, early uplift of the Tibetan Plateau, and reorganization of plate boundaries in the Indian Ocean. Sometime a little after 34 Ma, Greater India was consumed and thicker Indian Craton subsequently made contact with Asia, resulting in $\sim 6^\circ$ shortening or drifting northward of Asia. The model also provides a link between the timing of uplift of the Tibetan Plateau and global palaeoclimatic changes, namely for the Cenozoic global cooling that started at ~ 50 Ma⁵ and persisted during the Eocene-Oligocene transition (~ 34 Ma), as mountain building process and physical weathering of high plateau consume large quantity of CO₂⁵.

Methods

All demagnetization treatments and remanence measurements were performed in a shielded room with residual fields less than 300 nT at South China Sea Institute of Oceanology. Most of the samples were treated with stepwise thermal demagnetization. Some samples were also progressively demagnetized using alternating fields. The remanence after each step was measured on a 2G cryogenic magnetometer. Rock magnetic experiments were performed at the University of California, Santa Cruz. Magnetic hysteresis curves were measured on a Princeton Measurements MicroMag 2900 alternating gradient. The temperature versus susceptibility curves were measured using a Kappabridge KLY-2 susceptibility bridge with a CS-2 furnace.

Palaeomagnetic directions were identified using principal component analysis to obtain a best-fitting demagnetization trajectory⁵⁶. A few samples were analyzed with great circle methods⁵⁷. The formation means of best-fit directions were calculated using Fisher statistics⁵⁸, while those that included some great circles were calculated following McFadden & McElhinny (1988)⁵⁹. Confidence limits were calculated according to Coe *et al.* (1985)⁶⁰.

- Wang, C. S. *et al.* Constraints on the early uplift history of the Tibetan Plateau. *Proc. Natl Acad. Sci. USA* **105**, 4987–4992 (2008).
- Yin, A. & Harrison, T. M. Geologic evolution of the Himalayan-Tibetan orogen. *Annual Review of Earth and Planetary Sciences* **28**, 211–280 (2000).
- Molnar, P. & Tapponnier, P. Cenozoic tectonics of Asia: effects of a continental collision. *Science* **189**, 419–426 (1975).
- van Hinsbergen, D. J. J. *et al.* Restoration of Cenozoic deformation in Asia and the size of Greater India. *Tectonics* **30**, TC5003 (2011).
- Kent, D. V. & Muttoni, G. Equatorial convergence of India and early Cenozoic climate trends. *Proc. Natl Acad. Sci. USA* **105**, 16065–16070 (2008).
- Wang, C. *et al.* Revision of the Cretaceous-Palaeogene stratigraphic framework, facies architecture and provenance of the Xigaze forearc basin along the Yarlung Zangbo suture zone. *Gondwana Res.* **22**, 415–433 (2011).
- Durr, S. B. Provenance of Xigaze fore-arc basin clastic rocks (Cretaceous, south Tibet). *Geol. Soc. Am. Bull.* **108**, 669–684 (1996).
- Eisele, G. *et al.* The Xigaze forearc basin: evolution and facies architecture (Cretaceous, Tibet). *Sediment Geol.* **90**, 1–32 (1994).
- Patriat, P. & Achache, J. India-Eurasia collision chronology has implications for crustal shortening and driving mechanism of plates. *Nature* **311**, 615–621 (1984).
- Klootwijk, C. T., Gee, J. S., Peirce, J. W., Smith, G. M. & McFadden, P. L. An Early India-Asia Contact-Palaeomagnetic Constraints from Ninetyeast Ridge, ODP Leg 121. *Geology* **20**, 395–398 (1992).
- Najman, Y. The detrital record of orogenesis: A review of approaches and techniques used in the Himalayan sedimentary basins. *Earth-Sci. Rev.* **74**, 1–72 (2006).
- Najman, Y. *et al.* Timing of India-Asia collision: Geological, biostratigraphic, and palaeomagnetic constraints. *J. Geophys. Res.* **115**, B12416 (2010).
- van Hinsbergen, D. J. J. *et al.* Greater India Basin hypothesis and a two-stage Cenozoic collision between India and Asia. *Proc. Natl Acad. Sci. USA* **109**, 7659–7664 (2012).
- Aitchison, J. C., Davis, A. M., Badengzhu, B. & Luo, H. New constraints on the India-Asia collision: the Lower Miocene Gangrinboche conglomerates, Yarlung Tsangpo suture zone, SE Tibet. *J. Asian Earth Sci.* **21**, 251–263 (2002).
- Achache, J., Courtillot, V. & Xiu, Z. Y. Palaeogeographic and tectonic evolution of southern Tibet since middle Cretaceous time: New palaeomagnetic data and synthesis. *J. Geophys. Res.* **89**, 10311–10339 (1984).
- Liebke, U. *et al.* Position of the Lhasa terrane prior to India-Asia collision derived from palaeomagnetic inclinations of 53 Ma old dykes of the Linzhou Basin: constraints on the age of collision and post-collisional shortening within the Tibetan Plateau. *Geophys. J. Int.* **182**, 1199–1215 (2010).
- Dupont-Nivet, G., Lippert, P. C., van Hinsbergen, D. J. J., Meijers, M. J. M. & Kapp, P. Palaeolatitude and age of the Indo-Asia collision: palaeomagnetic constraints. *Geophys. J. Int.* **182**, 1189–1198 (2010).
- Chen, J. S., Huang, B. C. & Sun, L. S. New constraints to the onset of the India-Asia collision: Palaeomagnetic reconnaissance on the Linzong Group in the Lhasa Block, China. *Tectonophysics* **489**, 189–209 (2010).
- Tan, X. D. *et al.* New palaeomagnetic results from the Lhasa block: Revised estimation of latitudinal shortening across Tibet and implications for dating the India-Asia collision. *Earth Planet Sci. Lett.* **293**, 396–404 (2010).
- Sun, Z. M., Jiang, W., Li, H. B., Pei, J. L. & Zhu, Z. M. New palaeomagnetic results of Palaeocene volcanic rocks from the Lhasa block: Tectonic implications for the collision of India and Asia. *Tectonophysics* **490**, 257–266 (2010).
- Sun, Z. *et al.* Palaeomagnetism of late Cretaceous sediments from southern Tibet: Evidence for the consistent palaeolatitudes of the southern margin of Eurasia prior to the collision with India. *Gondwana Res.* **21**, 53–63 (2012).
- Aitchison, J. C. & Ali, J. R. India-Asia collision timing. *Proc. Natl Acad. Sci. USA* **109**, doi: 10.1073/pnas.1207859109 (2012).
- van Hinsbergen, D. J. J. *et al.* Reply to Aitchison and Ali: Reconciling Himalayan ophiolite and Asian magmatic arc records with a two-stage India-Asia collision model. *Proc. Natl Acad. Sci. USA* **109**, doi:10.1073/pnas.1208836109 (2012).
- Searle, M. *et al.* The closing of Tethys and the tectonics of the Himalaya. *Geol. Soc. Am. Bull.* **98**, 678–701 (1987).
- Ding, L., Kapp, P. & Wan, X. Q. Palaeocene-Eocene record of ophiolite obduction and initial India-Asia collision, south central Tibet. *Tectonics* **24**, 1–18 (2005).
- Li, J. G., Batten, D. J. & Zhang, Y. Y. Palynological indications of environmental changes during the Late Cretaceous-Eocene on the southern continental margin of Laurasia, Xizang (Tibet). *Palaeogeography, Palaeoclimatology, Palaeoecology* **265**, 78–86 (2008).
- Day, R., Fuller, M. & Schmidt, V. Hysteresis properties of titanomagnetites: grain-size and compositional dependence. *Phys. Earth Planet. In.* **13**, 260–267 (1977).
- Dunlop, D. J. Theory and application of the Day plot (Mrs/Ms versus Hcr/Hc) 1. Theoretical curves and tests using titanomagnetite data. *J. Geophys. Res.* **107**, B32056 (2002).
- McElhinny, M. Statistical significance of the fold test in palaeomagnetism. *Geophysical Journal of the Royal Astronomical Society* **8**, 338–340 (1964).
- Enkin, R. J. The direction-correction tilt test: an all-purpose tilt/fold test for palaeomagnetic studies. *Earth Planet Sci. Lett.* **212**, 151–166 (2003).
- McFadden, P. A new fold test for palaeomagnetic studies. *Geophys. J. Int.* **103**, 163–169 (1990).
- Ogg, J., Smith, A. G. in *A Geological Time Scale 2004* (ed Gradstein, F. M., Ogg, J. G., Smith, A. G.) 63–86 (Cambridge University Press, Cambridge, 2004).
- Tauxe, L. & Kent, D. V. A simplified statistical model for the geomagnetic field and the detection of shallow bias in palaeomagnetic inclinations: was the ancient magnetic field dipolar. *Timescales of the Palaeomagnetic field* **145**, 101–115 (2004).
- Lippert, P. C., Zhao, X., Coe, R. S. & Lo, C. H. Palaeomagnetism and 40Ar/39Ar geochronology of upper Palaeogene volcanic rocks from Central Tibet: implications for the Central Asia inclination anomaly, the palaeolatitude of Tibet and post-50 Ma shortening within Asia. *Geophys. J. Int.* **184**, 131–161 (2011).
- Copley, A., Avouac, J. P. & Royer, J. Y. India-Asia collision and the Cenozoic slowdown of the Indian plate: Implications for the forces driving plate motions. *J. Geophys. Res.* **115**, B03410 (2010).
- van Hinsbergen, D. J. J., Steinberger, B., Doubrovine, P. V. & Gassmoller, R. Acceleration and deceleration of India-Asia convergence since the Cretaceous: Roles of mantle plumes and continental collision. *J. Geophys. Res.* **116**, B06101 (2011).
- Molnar, P. & Stock, J. M. Slowing of India's convergence with Eurasia since 20 Ma and its implications for Tibetan mantle dynamics. *Tectonics* **28**, TC3001 (2009).
- Torsvik, T. H. *et al.* Phanerozoic polar wander, palaeogeography and dynamics. *Earth-Sci. Rev.* **114**, 325–368 (2012).
- Van der Voo, R. The reliability of palaeomagnetic data. *Tectonophysics* **184**, 1–9 (1990).
- Besse, J., Courtillot, V., Pozzi, J., Westphal, M. & Zhou, Y. Palaeomagnetic estimates of crustal shortening in the Himalayan thrusts and Zangbo suture. *Nature* **311**, 621–626 (1984).
- Tong, Y. *et al.* Early Palaeocene palaeomagnetic results from southern Tibet, and tectonic implications. *Int. Geol. Rev.* **50**, 546–562 (2008).
- Patzelt, A., Li, H. M., Wang, J. D. & Appel, E. Palaeomagnetism of Cretaceous to Tertiary sediments from southern Tibet: Evidence for the extent of the northern margin of India prior to the collision with Eurasia. *Tectonophysics* **259**, 259–284 (1996).
- Yi, Z., Huang, B., Chen, J., Chen, L. & Wang, H. Palaeomagnetism of early Palaeogene marine sediments in southern Tibet, China: Implications to onset of the India-Asia collision and size of Greater India. *Earth Planet Sci. Lett.* **309**, 153–165 (2011).
- Pozzi, J. P., Westphal, M., Zhou, Y. X., Xing, L. S. & Chen, X. Y. Position of the Lhasa block, South Tibet, during the late Cretaceous. *Nature* **297**, 319–321 (1982).
- Westphal, M., Pozzi, J. P., Zhou, Y. X., Xing, L. S. & Chen, X. Y. Palaeomagnetic data about southern Tibet (Xizang)—The Cretaceous formations of the Lhasa block. *Geophysical Journal of the Royal Astronomical Society* **73**, 507–521 (1983).
- Lin, J. L. & Watts, D. R. Palaeomagnetic results from the Tibetan Plateau. *Phil. Trans. R. Soc. A, Mathematical and Physical Sciences* **327**, 239–262 (1988).
- Johnson, C. *et al.* Recent investigations of the 0–5 Ma geomagnetic field recorded by lava flows. *Geochem. Geophys. Geosyst.* **9**, Q04032 (2008).
- Biggin, A. J., van Hinsbergen, D. J. J., Langereis, C. G., Straathof, G. B. & Deenen, M. H. L. Geomagnetic secular variation in the Cretaceous Normal Superchron and in the Jurassic. *Phys. Earth Planet. In.* **169**, 3–19 (2008).
- He, S. D., Kapp, P., DeCelles, P. G., Gehrels, G. E. & Heizler, M. Cretaceous-Tertiary geology of the Gangdese Arc in the Linzhou area, southern Tibet. *Tectonophysics* **433**, 15–37 (2007).



50. Capitanio, F. A., Morra, G., Goes, S., Weinberg, R. F. & Moresi, L. India-Asia convergence driven by the subduction of the Greater Indian continent. *Nature Geosci.* **3**, 136–139 (2010).
51. Leloup, P., Tapponnier, P., Lacassin, R. & Searle, M. Discussion on the role of the Red River shear zone, Yunnan and Vietnam, in the continental extrusion of SE Asia Journal, Vol. 163, 2006, 1025–1036. *J. Geol. Soc. Lond.* **164**, 1253–1260 (2007).
52. Ran, B. *et al.* Dimension of Greater India in the early Mesozoic: palaeomagnetic constraints from Triassic sediments in the Tethyan Himalaya. *J. Asian Earth. Sci.* **53**, 15–24 (2011).
53. Wang, J. G., Hu, X. M., Jansa, L. & Huang, Z. C. Provenance of the Upper Cretaceous-Eocene Deep-Water Sandstones in Sangdanlin, Southern Tibet: Constraints on the Timing of Initial India-Asia Collision. *J. Geol.* **119**, 293–309 (2011).
54. Guillot, S., Mahéo, G., De Sigoyer, J., Hattori, K. & Pêcher, A. Tethyan and Indian subduction viewed from the Himalayan high-to ultrahigh-pressure metamorphic rocks. *Tectonophysics* **451**, 225–241 (2008).
55. Copley, A., Avouac, J. P. & Wernicke, B. P. Evidence for mechanical coupling and strong Indian lower crust beneath southern Tibet. *Nature* **472**, 79–81 (2011).
56. Kirschvink, J. The least-squares line and plane and the analysis of palaeomagnetic data. *Geophysical Journal of the Royal Astronomical Society* **62**, 699–718 (1980).
57. Halls, H. The use of converging remagnetization circles in palaeomagnetism. *Phys. Earth Planet In.* **16**, 1–11 (1978).
58. Fisher, R. Dispersion on a sphere. *Proc. R. Soc. A. Mathematical and Physical Sciences* **217**, 295–305 (1953).
59. McFadden, P. & McElhinny, M. The combined analysis of remagnetization circles and direct observations in palaeomagnetism. *Earth Planet Sci. Lett.* **87**, 161–172 (1988).
60. Coe, R. S., Globerman, B. R., Plumley, P. W. & Thrupp, G. A. Palaeomagnetic results from Alaska and their tectonic implications. in *Tectonostratigraphic terranes of the Circum-Pacific region: American Association of Petroleum Geologists* (ed Howell, D. G.) 85–108 (Circum-Pacific Council on Energy and Resources Earth Sciences Series, 1985).

Acknowledgements

We thank Dr. Gaojun Li and the three journal reviewers for the helpful reviews and constructive suggestions that greatly improved the original manuscript. We also thank Drs. Xiaodong Tan, Xianghui Li, Xiumian Hu, Peter Lippert, Yulin Han, Jiangang Wang for discussions and acknowledge the help of many colleagues in carrying out the field work and lab measurements: Ms. Yan Chen, Mr. Long Li, Mr. Dylan Tabor, Mr. Kai Luo, Mr. Nuoya Sun, and Mr. Baoseng Zhang. This study has been supported by the National Basic Research Program of China (2012CB822000), National Natural Science Foundation of China (41072075 and 40974035), Zhongba 1:50,000 geological mapping projects by Chinese Bureau of Geological Survey (12112011086037), China Scholarship Council Scholarship Program, the fundamental research funds for the central universities of China (2-9-2011-162), the US National Science Foundation grant EAR-0911331, and 111 Project of China Grant (B07011).

Author contributions

C.S.W designed the study. J.M. performed the palaeomagnetic sampling and measurements. Y.L.L. contributed field study. D.F. helped with lab work. J.M., C.S.W., X.Z., R.S.C., Y.L.L. and D.F. performed data analyses and wrote the paper.

Additional information

Supplementary information accompanies this paper at <http://www.nature.com/scientificreports>

Competing financial interests The authors declare no competing financial interests. Correspondence and requests for materials should be addressed to J.M. and C.S.W.

License: This work is licensed under a Creative Commons Attribution-NonCommercial-NoDerivs 3.0 Unported License. To view a copy of this license, visit <http://creativecommons.org/licenses/by-nc-nd/3.0/>

How to cite this article: Meng, J. *et al.* India-Asia collision was at 24°N and 50 Ma: palaeomagnetic proof from southernmost Asia. *Sci. Rep.* **2**, 925; DOI:10.1038/srep00925 (2012).